THE DESIGN AND APPLICATION OF NICKEL–CADMIUM BATTERIES IN SPACE

GERALD HALPERT

Jet Propulsion Laboratory, California Institute of Technology, 4800 Oak Grove Drive, Pasadena, CA 91109 (U.S.A.)

(Accepted March 12, 1985)

Summary

This paper describes the considerations given to selection of 20 and 50 A h nickel–cadmium cells and batteries for NASA/Goddard Space Flight Center's Solar Max and Landsat D Missions. Results of cell and battery manufacturer testing and improvements in design required by the NASA standard specifications are shown. Operation of 3 batteries in parallel using a single voltage limit/current taper charge control system is described along with suggestions for optimizing life and uniformity. The result of 3 years of in-orbit operation is presented.

Introduction

The concept that an electrochemical cell is treated as a part, *i.e.*, resistor, capacitor, etc., has been expressed by those unfamiliar with electrochemical technology. Those of us in the electrochemical cell and battery community are well aware that the performance of a battery is based on the complex electrochemistry and physical chemistries involved in cell and battery operation. The complexities must be taken into consideration in the design and use of nickel–cadmium batteries for long term reliable use in an aerospace application. This paper will describe the fundamentals of design, and examples of use, of nickel–cadmium batteries in space. It will also cover the parameters and evaluation data utilized in cell/battery selection, and results of some recent flight missions.

These results refer to NASA Standard 20 A h cells and batteries in the Solar Max Mission (SMM) Spacecraft and 50 A h cells and batteries in the Landsat D Spacecraft. The requirements, selection, and performance of several lots of plate materials, and the cells and batteries from which they are made, will be described together with in-orbit data relating to the degree of uniformity maintained for more than 4 years.

0378-7753/85/$3.30

The results achieved in this effort have been made possible by the following:

(a) experience with the relationship between the manufacturing variables and the final cell/battery characteristics;

(b) control of the materials and process of manufacture despite the complexity involved with manufacturing;

(c) a good working relationship between cell manufacturer (General Electric), battery manufacturer (McDonnell Douglas Astronautics), user (General Electric and Fairchild), and the government technical representatives.

The cells described are manufactured by General Electric to specifically documented Manufacturing Control Documents. The 20 A h cells are designated 42B024AB06 (07 for signal electrode cell). The 50 A h cells are designated 42B050AB20 (21 for signal electrode cell). Both types are assembled according to Manufacturing Control Document (MCD) No. 232A2222-AA-84. The plate materials are essentially those from GE's commercial operation, with some additional quality steps to optimize uniformity. The plate materials, as well as the other cell components — separator, case, covers, etc. — are eventually incorporated into the sealed cell in the G. E. Aerospace Facility. It is in this operation where the material testing and selection and cell assembly take place. The cells, prior to delivery, are subjected to a number of tests culminating in four cycles at three temperatures required for NASA acceptance.

The cells are then delivered to McDonnell Douglas to be selected, installed, and tested in a battery for satellite power system use. The standard 20 A h battery is designated 70A237003 and the 50 A h battery 70A237005. They are assembled and tested according to BMCD 70A237003 and BMCD 70A237005, respectively.

Several improved design features, and unique procedures utilized in the production of the cells and batteries, were implemented to improve their uniformity and operational life. These are given in Tables 1 and 2.

A complete description of the battery design is provided in the Standard 20 A h Battery Manual [1] and 50 A h Battery Manual [2].

TABLE 1

Cell design features of NASA Standard Cell

Lighter loaded plates (10 - 15%)
Additional electrolyte (20%)
Material buyoff review
Flooded plate stability tests
Burn-in test requirement
Standard Cell NASA/GSFC Acceptance Test — no rework
Capacity of 24 ± 2 A h and 60 ± 5 A h at 24 °C
No optimization of energy density

TABLE 2

Battery design features

Battery Manufacturing Control Document (BMCD)
Selection of cells from GE data only
Normalization of manufacturer data
22 cells for battery selected from 25 cell lot
Standard Battery Flight Qualification and Acceptance Tests

A complete description of the battery design is provided.

Mission application

The mission applications of these cells and batteries are described in Fig. 1. The important feature is that the three batteries in each case were tied to the same bus, charged, and discharged in parallel. The second important feature is the charge control method, voltage limit (temperature compensated)/current taper, which our experience tells us optimizes life of nickel–cadmium cells and batteries.

The in-orbit cell and battery parameters that affect operation and life are given in Fig. 2. All are functions of the cell design which determine cell characteristics.

	SOLAR MAX MISSION	LANDSAT-D
BATTERIES	3	3
CELLS/BATTERY	22	22
CELL/TYPE	20AH NASA STANDARD	50AH NASA STANDARD
OPERATION	BATTERIES IN PARALLEL	BATTERIES IN PARALLEL
BUS	COMMON BUS/NO DIODES	COMMON BUS/NO DIODES
CHARGE CONTROL	V LIMIT/I TAPER	V LIMIT/I TAPER
LAUNCHED	FEBRUARY 1980	AUGUST 1982

Fig. 1. The SMM and Landsat D applications.

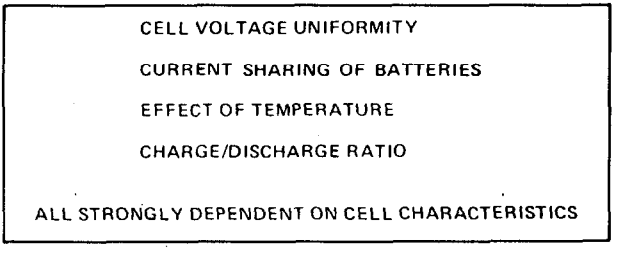

Fig. 2. In-orbit battery performance concerns.

Cell design and uniformity

The material buyoff review was instituted with the development of the Standard Cells. In addition to plate loading and dimensional characteristics, the parameters described in Fig. 3 were reviewed. Continuation of the cell assembly operations was dependent on the results of this review. Three lots of material had been rejected at this point in the process. Specific data for acceptable flight lots will be discussed in the following Figures.

The cell design limits are given in Fig. 4. The plate physical characteristics, including loading levels, are given in Table 3.

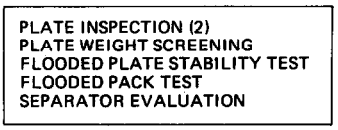

Fig. 3. Material buyoff review.

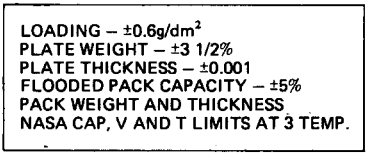

Fig. 4. Cell design limits.

TABLE 3

Plate characteristics

	20 A h Cell		50 A h Cell	
	+	–	+	–
No. of plates	10	11	15	16
Loading (g/dm²)	11.60	15.25	12.50	16.06
Loading (g/cc void)	1.8	2.5	2.3	2.8
Porosity (%)*	89	89	89	86
Plate thickness (mil)	27	31	27	31

*Without substrate.

The loading, given in g/dm², was the manufacturer limits, and the g/cc void values were determined analytically. The capacity measurements were made at 24, 0, and 35 °C and then again at 24 °C. Each had appropriate voltage and measurement requirements given in the cell specifications [3].

The values for loading, measured pack electrochemical test capacity, and utilization are given in Figs. 5 and 6. The uniformity is quite good for the three parameters of the cell plate lots given. The 8A and 8B plate lots in Fig. 5 have a lower than average loading (but within the acceptable range) and a higher than average utilization. The capacity of the lot nine positives was high and reflected the maximum loading level and a high utilization. The negatives had utilization as high as 88 percent.

The results of the plate stability test are given in Figs. 7 and 8. Five samples of positive plates from the entire lot are charged in the flooded condition at $C/5$ for eight hours and discharged at $C/2$ to 0.0 V for five

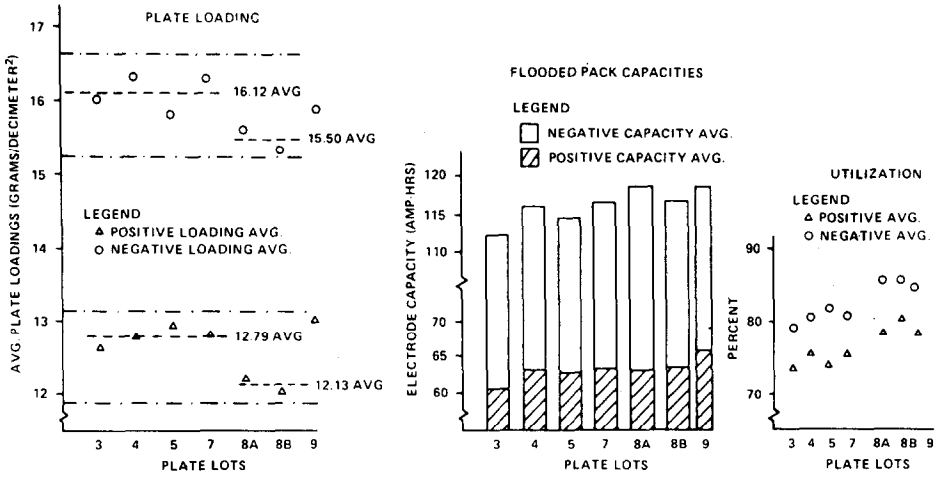

Fig. 5. 50 A h Summary plate and pack data.

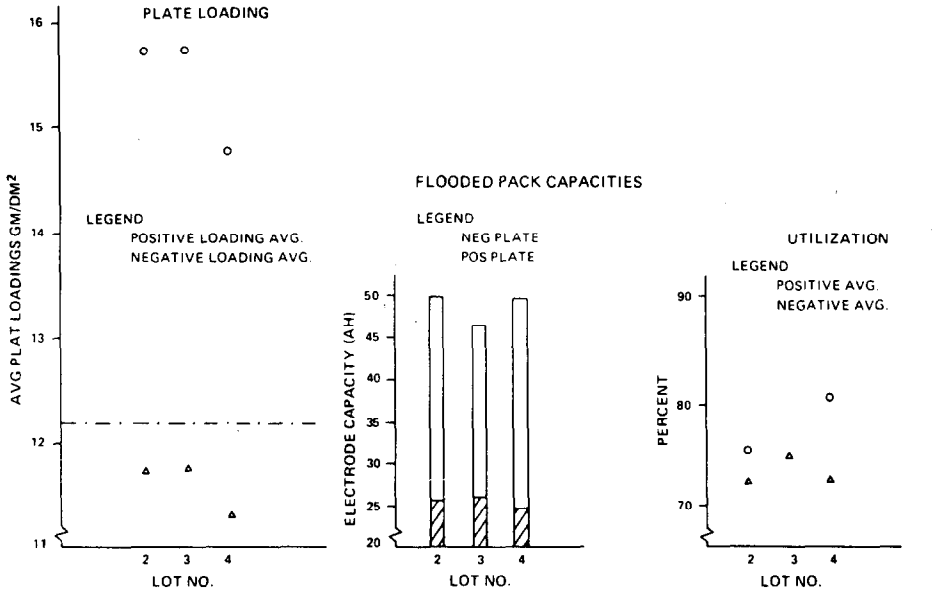

Fig. 6. 20 A h Summary plate and pack data.

consecutive orbits. Five negative plates are charged in the flooded condition at $C/2$ for five hours and discharged at $C/2$ to 0.0 V for 20 cycles. There is a requirement that the 20th cycle capacity be within 75% of the second cycle capacity. There is an initial conditioning cycle for each plate. The results are quite consistent except for the lot 8A and 8B plates. The unusual behavior of the 8A and 8B plates in the 50 A h cell plates (see Fig. 7), when compared with the others, led to the conclusion that these plates may have

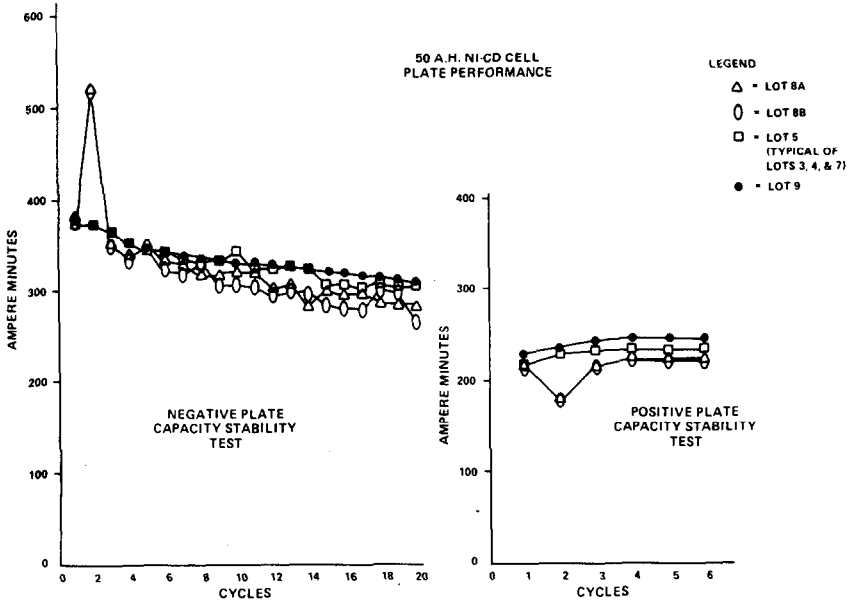

Fig. 7. Plate stability test results (50 A h).

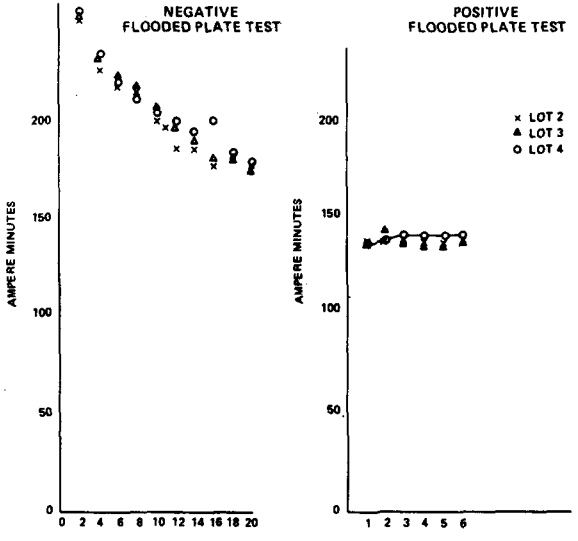

Fig. 8. Plate stability test results (20 A h).

been subjected to an unusual condition(s) during manufacture, and they were rejected.

The plate weight screening results are given in Fig. 9. The average weight of each 20 A h and 50 A h plate lot is given, as is the ± 3-1/2% range of weight acceptable for use. This go/no go test is done by utilizing two balances, one set for the upper and the other for the lower weight. The

PLATE WEIGHT SCREENING

NASA STANDARD 20AH CELLS

LOT	POSITIVE PLATES AVG. WEIGHT (G)	POSITIVE PLATES ±3-1/2% WEIGHT (G)	POSITIVE PLATES % REJECTED HIGH/LOW	NEGATIVE PLATES AVG. WEIGHT (G)	NEGATIVE PLATES ±3-1/2% WEIGHT (G)	NEGATIVE PLATES % REJECTED HIGH/LOW
1	23.14	0.81	0/1.7	28.50	1.00	/0
2	23.34	0.83	6.2/3.1	29.83	1.05	0/0.3
3	22.95	0.80	6.3/4.4	28.86	1.02	0.2/2.0
4	22.95	0.80	4.4/3.0	28.85	1.01	0.2/9.0
			NASA 50AH CELLS			
1	35.65	1.25	3.2/6.7	45.51	1.60	0.8/1.4
3	35.81	1.26	2.2/0.3	46.02	1.62	0/4.5
4	35.82	1.25	5.6/3.5	45.96	1.61	.1/0
5	36.88	1.29	1.7/0	45.60	1.60	0/0
7	36.59	1.29	0/2.3	46.18	1.61	0/2.4
9	37.96	1.32	3.1/0	45.44	1.59	0.2/0.7

Fig. 9. Plate weight screening.

PLATE LOT	MAX THEORETICAL CAP.* POSITIVE	MAX THEORETICAL CAP.* NEGATIVE	FLOODED CELL AVG. CAP. POS/% THEO.	FLOODED CELL AVG. CAP. NEG/% THEO.	SEALED AVG. CAP. TO IV/CELL	SEALED AVG. CAP. % FLOODED	NEG TO POS RATIO
1	83.43 AH	143.39 AH	64.30/77.0	118.69/82.7	62.76 AH	97.6	1.84
2	82.38 AH	143.22 AH	64.80/78.6	120.58/84.2	59.80 AH	92.3	1.86
3	83.03 AH	141.72 AH	60.76/73.2	112.08/79.1	60.14 AH	99.0	1.85
4	83.95 AH	144.46 AH	63.20/75.3	116.37/80.5	60.28 AH	95.4	1.84
5	85.21 AH	139.94 AH	62.78/73.7	114.47/81.8	55.54 AH	88.5	1.82
7	84.15 AH	144.19 AH	63.40/75.3	116.63/80.8	61.07 AH	96.3	1.84

* BASED ON AVG PLATE LOADING.

Fig. 10. 50 A h Cell active material utilization summary.

total number of plates rejected for high and low weight are, with one exception, significantly less than five percent. of the total screened. The importance of this quality screening test is based on the relationship between plate weight and plate capacity, described previously [4].

The 50 A h pack capacities, theoretical and flooded, are compared in Fig. 10. The uniformity again is obvious. The pack capacities performed to a specific requirement in the MCD are determined by discharging through a load bank which will have an apparent effect on uniformity. The 1:8 negative-to-positive plate ratio is quite consistent.

Battery design and uniformity

The limitations and requirements on battery manufacture are given in Fig. 11. There are twenty-two series-connected cells (see Fig. 12) including one with a signal electrode used to monitor relative internal oxygen pressure.

SELECT CELLS ON CELL MFG. RESULTS
CAPACITIES – ±3%
CELL VOLTAGE – ±0.008V
BATTERY MATCHING – ±5%
MAX VOLTAGE AT 0 °C and 24 °C
PEAK LOAD 3C FOR 5 MINUTES – 50% DOD
THERMAL GRADIENT
±1.5 °C PARALLEL TO COVER
5 °C ABOVE BASEPLATE

Fig. 11. Limits on battery manufacturers.

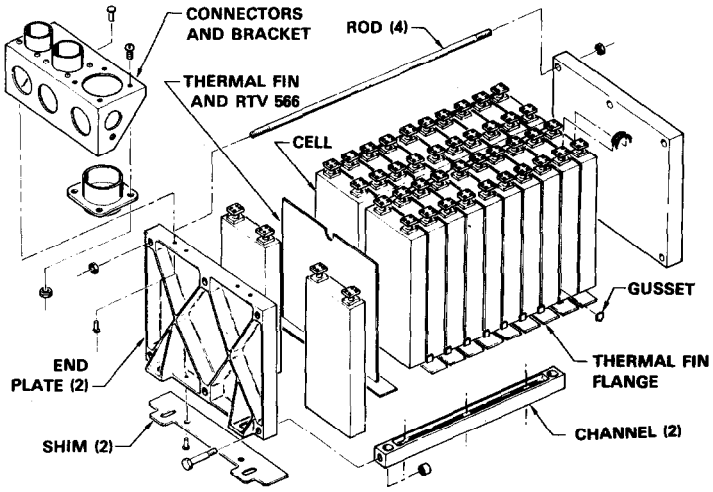

Fig. 12. Battery mechanical/structural design.

The design of the battery is described in detail in refs. 1 and 2. The design requirements are given in Fig. 11 and include also those features given in Table 4.

After normalizing the cell manufacturers' capacity and voltage data for each lot, the average high and low differences are determined. These

TABLE 4

Battery evaluation tests

(a) Selection of cells based on cell manufacturer data
(b) Selection of ± 3% of capacity at 24 and 0 °C
(c) Cell voltage range ± 8 mV at 24 and 0 °C
(d) Battery capacity 90% of average manufacturer cell capacity at 20 °C
Battery capacity 85% of average manufacturer cell capacity at 10 °C
Battery capacity 80% of average manufacturer cell capacity at 0 °C
(e) Capacity ± 5% between batteries
(f) Peak load 3*C* for 5 minutes at 50% discharged
(g) Normalization of cell manufacturer data for selection
(h) Selection of 22 cells from 25 cell lot

are given in Fig. 13. The capacities are all within the required range as is the voltage at 0 and 24 °C.

Battery testing includes 25% depth of discharge operation at 0, 10 and 20 °C in the voltage limit/current, taper mode. Comparison of eight 50 A h batteries tested individually at different time periods is given in Fig. 14. The maximum difference in end of discharge voltage (EODV) between all eight batteries was 0.1 V at 0 °C. The maximum difference in end of charge

	24°C CAPACITY		24°C VOLTAGE		0°C CAPACITY		0°C VOLTAGE	
BTRY NO.	HI-AVG	LO-AVG	HI-AVG	LO-AVG	HI-AVG	LO-AVG	HI-AVG	LO-AVG
1	+1.7%	-2.8%	+5.2 MV	-2.8 MV	+3.6%	-3.1%	+5.9 MV	-4.0 MV
2	+2.9%	-1.9%	+6.1 MV	-9 MV	+2.4%	-2.2%	+6.7 MV	-5.3 MV
3	+1.6%	-1.3%	+4.2 MV	-7.9 MV	+1.3%	-1.1%	+5.1 MV	-3.8 MV
4	+2.8%	-3.0%	+4.8 MV	5.3 MV	+3.0%	-5.8%	+6.8 MV	-7.2 MV
5	+1.8%	-1.6%	+4.8 MV	-4 MV	+1.3%	-1.4%	+5.3 MV	-3.5 MV
6	+1.2%	-1.2%	+3.8 MV	-5.2 MV	+4.9%	-2.3%	+6.4 MV	-5.6 MV
7	+1.7%	-2.7%	+4.3 MV	-4.7 MV	+2.4%	-2.3%	+4.5 MV	-3.6 MV
8	+1.0%	-3.4%	+3.9 MV	-5.1 MV	+2.9%	-2.8%	+3.9 MV	-6.1 MV
9	+1.8%	-1.8%	+6.4 MV	-5.6 MV	+2.7%	-2.6%	+5.3 MV	-6.7 MV
10	+2.1%	-2.3%	+4.7 MV	-6.3 MV	+3.1%	-2.7%	+6.1 MV	-10.2 MV
11	+2.0%	-2.0%	+3.1 MV	-2.9 MV	+2.7%	-2.6%	+3.5 MV	-7.5 MV
12	+3.0%	-2.9%	+6.7 MV	-3.3 MV	+2.2%	-2.5%	+7.2 MV	-4.5 MV
13	+1.6%	-1.2%	+3.6 MV	-4.6 MV	+2.2%	-1.7	+4.6 MV	-6.5 MV
14	+2.0%	-1.3%	+2.0 MV	-3.0 MV	+1.4%	-1.4%	+3.8 MV	-4.7 MV

Fig. 13. Normalized 50 A h cell matching summary.

CYCLING TESTS			
0°C CYCLING, 25% DOD, 5TH CYCLE			
	EODV	EOCV	EOCI
MAX	27.957	32.618	2.045
MIN	26.057	32.553	1.516
Δ	0.100	.065	0.529
10°C CYCLING, 25% DOD, 5TH CYCLE			
	EODV	EOCV	EOCI
MAX	27.100	32.088	2.092
MIN	27.021	32.046	1.786
Δ	0.079	0.042	0.306
20°C CYCLING, 25% DOD, 5TH CYCLE			
	EODV	EOCV	EOCI
MAX	27.078	31.542	2.980
MIN	27.006	31.521	2.589
Δ	0.072	0.021	0.391
3C PULSE (AFTER 1 HR DISCH.)			
MAX	23.448		
MIN	23.306		
Δ	0.142		

Fig. 14. Max/min variations, 8 - 50 A h batteries flight acceptance.

voltage (EOCV) fixed by the power supplies is given to provide a measure of the variation in test conditions and equipment.

The end of charge current values are also given. Here, differences in temperature and charge voltage add to the effect of differences in cell material properties and internal impedance. Differences in battery voltage measured at the end of the $3C-5$ minute pulse are also given.

The results of the capacity tests and the EOCV, after one hour of discharge at $C/2$ are given for the 24, 0 and 10 °C capacity tests on the eight batteries in Fig. 15. The uniformity is quite apparent, as is that given for similar cycling and capacity tests on the 20 A h batteries in Figs. 16 and 17.

MDAC FLIGHT ACCEPTANCE TESTS
CAPACITY TESTS

24°C CAPACITY

	EOCV	1HR C/2 DISCH V	CAPACITY
MAX	32.525	27.132	61.283
MIN	32.445	27.072	58.126
Δ	0.080	0.060	3.257

0°C CAPACITY

	EOCV*	1HR C/2 DISCH V	CAPACITY
MAX	32.243	27.012	57.53
MIN	33.036	26.808	49.11
Δ	0.207	0.204	8.42

10°C CAPACITY

	EOCV*	1HR C/2 DISCH V	CAPACITY
MAX	32.627	27.098	58.63
MIN	32.495	27.001	51.16
Δ	0.032	.097	7.47

*CONTROLLED BY POWER SUPPLY

Fig. 15. Max/min variations, 50 A h batteries capacity tests.

20AH BATTERIES – MDAC FLIGHT ACCEPTANCE
CYCLING TESTS

0°C CYCLING, 25% DOD, 5TH CYCLE

	EOD	EOCV	EOCI
MAX	27.246	32.594	.700
MIN	27.205	32.588	.690
Δ	.041	.006	.010

10°C CYCLING, 25% DOD, 5TH CYCLE

	EODV	EOCV	EOCI
MAX	27.286	32.080	.831
MIN	27.263	32.064	.800
Δ	.023	0.016	.031

20°C CYCLING, 25% DOD, 5TH CYCLE

	EODV	EOCV	EOCI
MAX	27.238	32.553	1.233
MIN	27.218	31.544	1.133
Δ	.020	.009	0.100

Fig. 16. Max/min variations, 3 flight batteries SMM.

MDAC FLIGHT ACCEPTANCE TESTS
CAPACITY TESTS

24° CAPACITY

	EOCV	1HR DISCH V	CAPACITY
MAX	32.292	27.409	24.194
MIN	32.147	27.338	23.332
Δ	0.145	0.071	0.862

0°C CAPACITY

	EOCV	1HR DISCH V	CAPACITY
MAX	33.019	27.324	22.097
MIN	32.997	27.109	21.119
Δ	0.022	0.225	0.978

10°C CAPACITY

	EOCV	1HR DISCH V	CAPACITY
MAX	32.445	27.306	22.435
MIN	32.388	27.280	21.962
Δ	0.057	0.026	0.473

3C PULSE (AFTER 1 HR DISCH.)

MAX	24.517
MIN	23.795
Δ	0.722

Fig. 17. Max/min variations, 20 A h batteries capacity tests.

Battery charge control/management

The technique used for charge control was adopted from the Orbiting Astronomical Observatory (OAO) spacecraft power system — a GSFC launch in the late 60s that lasted eight years in orbit. The charge control/management technique (Fig. 18) utilizes a temperature compensated-voltage (V_t) limit to reduce the charge current from a maximum (available from the solar array minus the load) to a relatively low taper current at the end of the daylight period. The power system configuration is shown in Fig. 19. The Standard Power Regulator Unit (SPRU) controls the V_t level and power available to charge the battery. A third electrode cell in each battery

TECHNIQUES/METHODS USED

- VOLTAGE LIMIT TEMPERATURE COMPENSATED (VT)
- CURRENT LIMIT
- COULOMETER
  - ELECTROCHEMICAL
  - ELECTRONIC AMPERE-HOUR METER
- THIRD ELECTRODE
- COMBINATIONS OF ABOVE

COMMONALITY OF TECHNIQUES

- CONTROL THE CHARGE TO DISCHARGE RATIO (C/D)
  - STATE OF CHARGE VS. C/D RATIO

Fig. 18. Battery charge control/management.

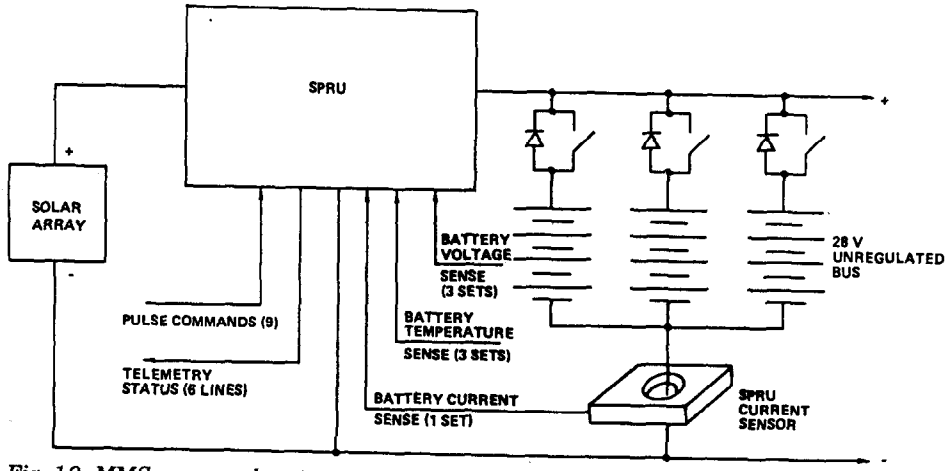

Fig. 19. MMS power subsystem configuration.

serves as an overcharge indicator, providing information on the increase of cell pressure at the end of charge.

The voltage limit temperature curves used on the MMS and other NASA spacecraft are shown in Fig. 20. The slopes represent the effect of tempera-

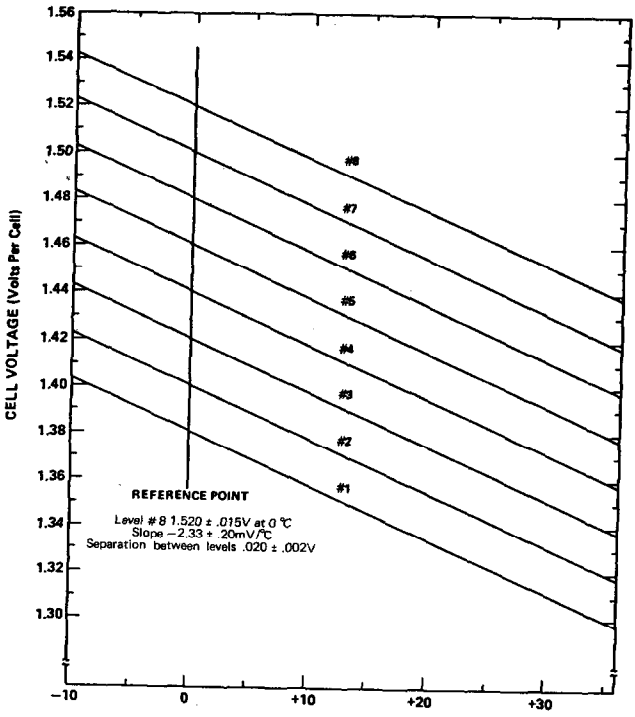

Fig. 20. Voltage/temperature characteristics for multilevel nickel–cadmium battery charging.

ture on voltage. For the case of a 25% Depth of Discharge (DOD) in a 65 min daylight/35 min night, orbit Level 5 has been found to be adequate. Testing in this manner has resulted in greater than 25 000 cycles (5 years) without failure.

Optimizing the amount of charge is always a concern. There has to be enough overcharge to top off the batteries in a uniform way and yet not sufficiently excessive so that heat and degradation are minimized. It is known that as temperature increases, there is an increase in inefficiency on charge. To account for this, a curve of C/D ratio *vs.* temperature must also be considered (Fig. 21). This curve provides the range of C/D ratios that are acceptable. It indicates that a C/D ratio of 1.05 - 1.08 is required for 10 °C whereas at 25 °C the C/D ratio should be 1.12 - 1.15. The higher the ratio, the greater the overcharge and the amount of heat that must be dissipated.

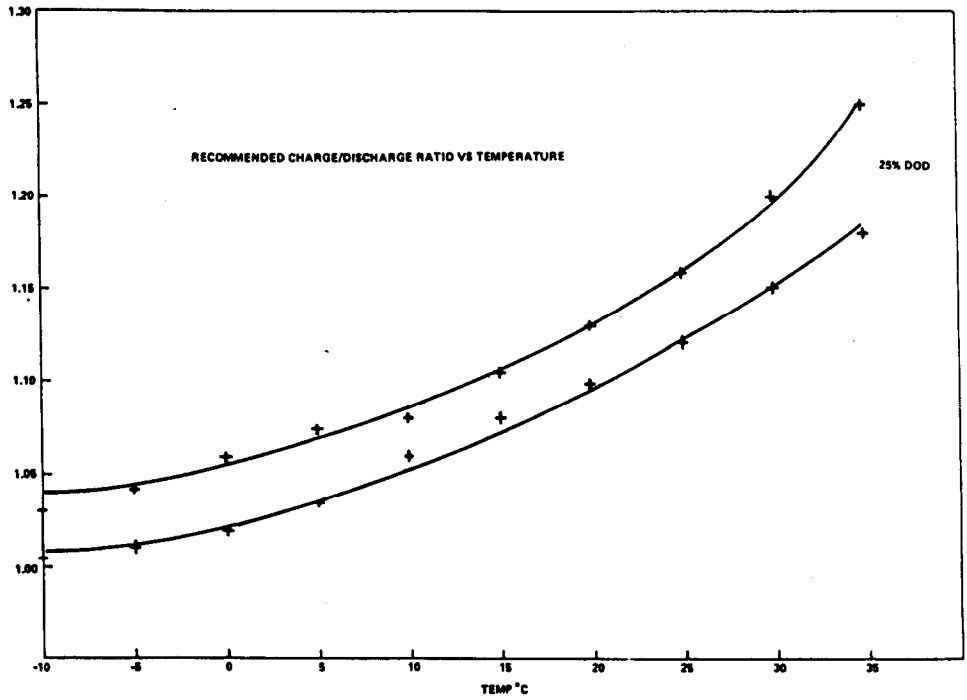

Fig. 21. Recommended charge/discharge ratio *vs.* temperature.

Figures 22 and 23 are typical voltage, current, and temperature characteristics using V_T5 at 10 °C and V_T7 at 20 °C during the parallel battery test effort at GSFC [7]. Note the current in this case is limited to 6 A which, for these 12 A h test cells, is the $C/2$ rate. The discharge is also at the $C/2$ rate. When the voltage reaches Level 5 (Fig. 9) or Level 7 (Fig. 10), the current drops, while the voltage of the cell remains constant. The higher voltage of

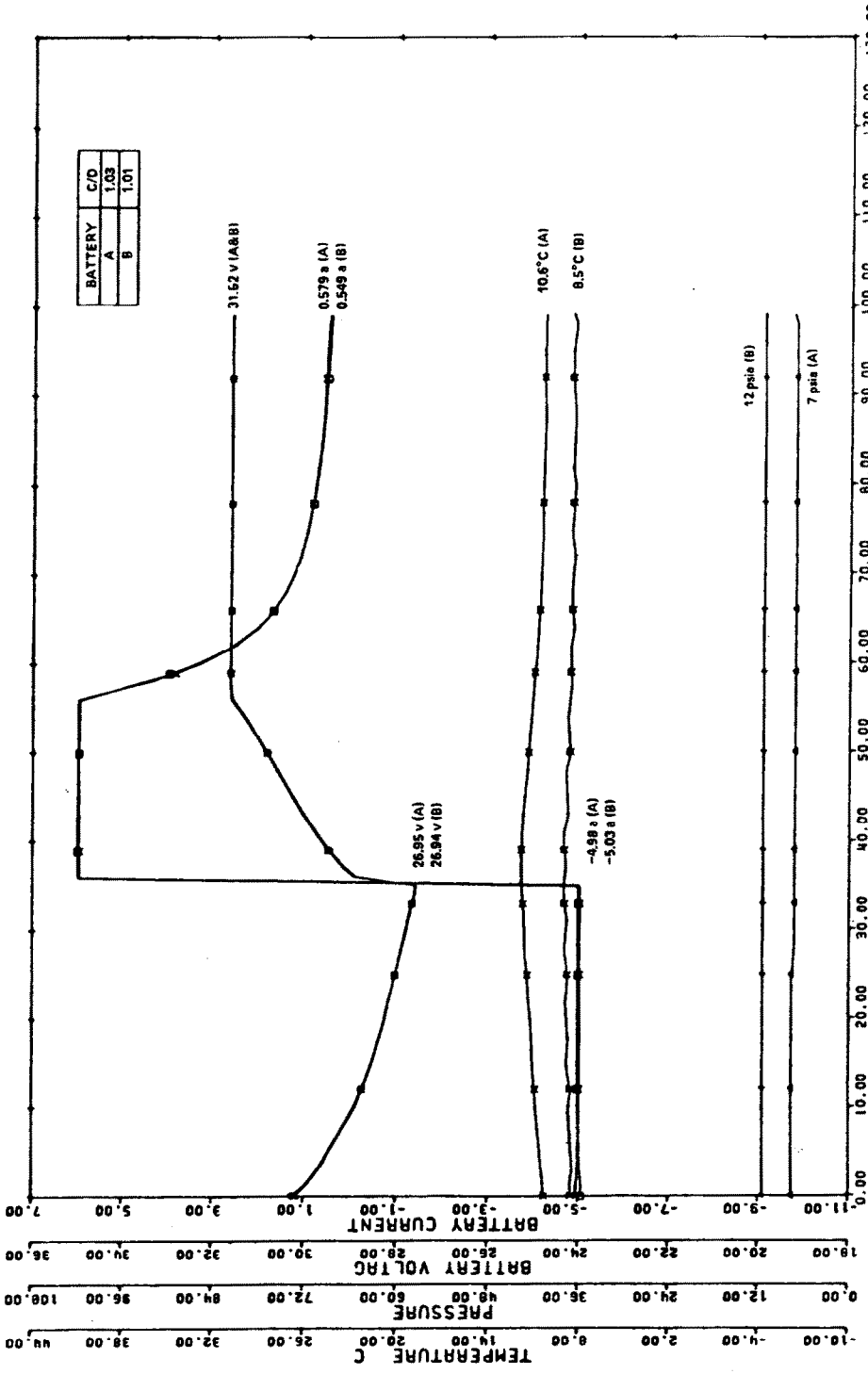

Fig. 22. Battery charge response at Level 5 and 10 °C.

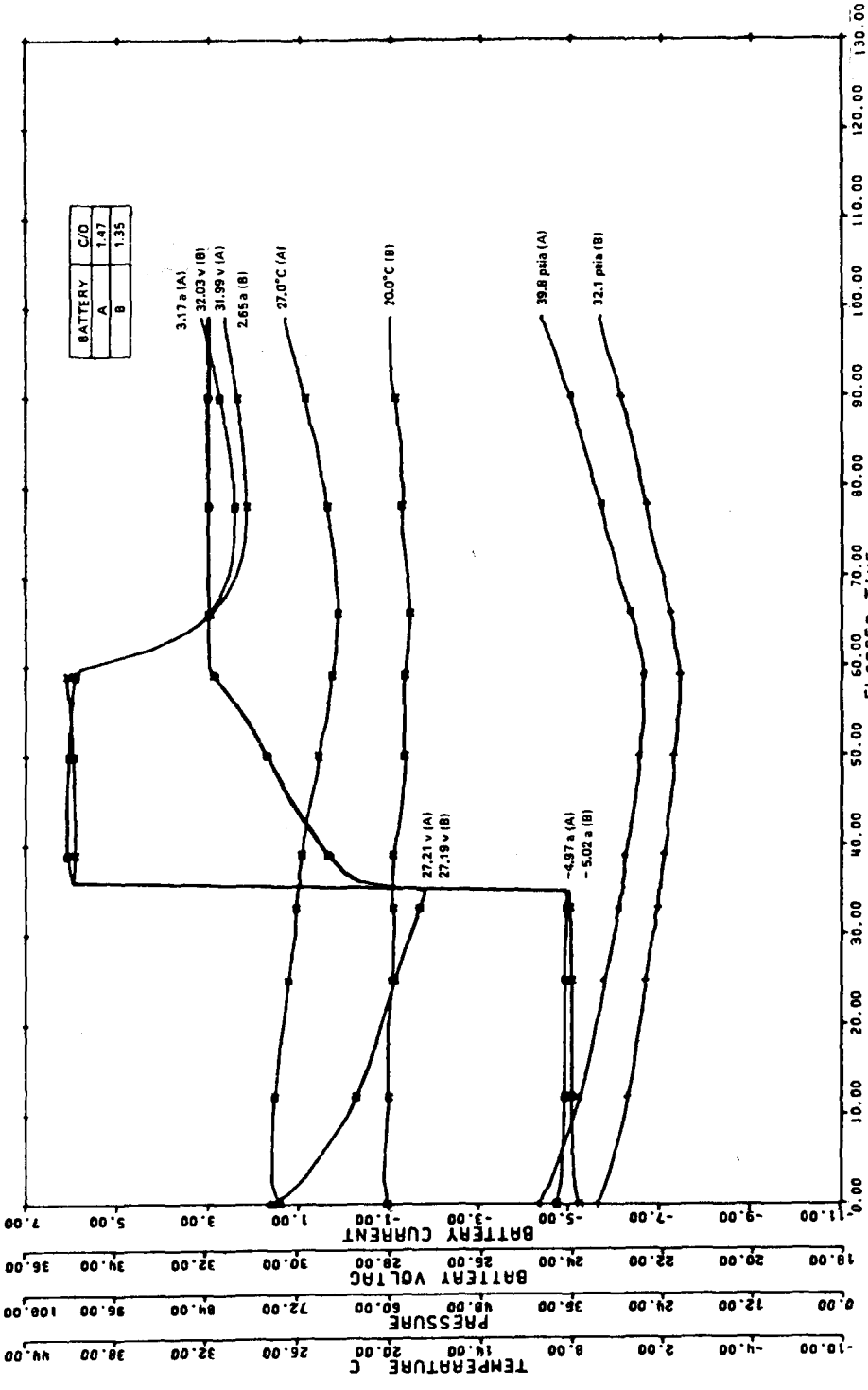

Fig. 23. Battery charge response at Level 7 and 20 °C.

Level 7 allows the maximum current to continue longer, so that when the V_T level is reached the ampere hour input to that point is higher than Level 5. This also results in a higher taper current for the 25% DOD discharge which, because of the associated increase in the heating during overcharge, can lead to thermal runaway. This is noted by the increasing current at the end of charge at Level 7 but not at Level 5.

The data from the 15 year NASA test program at the Naval Weapons Support Center (NWSC) [8, 9] at Crane, Indiana, has been compiled along with flight data from several NASA/GSFC missions. The projected life is shown in Fig. 24 [10]. Near Earth (65/35) orbits at 0 and 20 °C are given along with geosynchronous mission results at 10 - 15 °C.

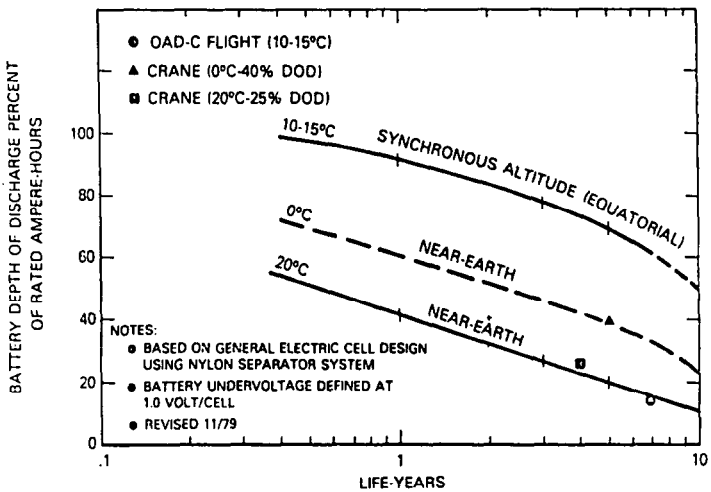

Fig. 24. Maximum design utilization of nickel–cadmium batteries for spacecraft applications (demonstrated capability).

Landsat D results

The evidence of operational uniformity on orbit 1251 of the Landsat D spacecraft, launched in July, 1982, is shown in the next several figures. Figure 25 provides data from the high current sensors (±50 A) and Fig. 26 from the low current sensors (0 - 3 A) for each battery. The current sharings by the three batteries is a measure of the uniformity of operation of the cells and the parallel batteries. Differences in cell properties will affect the battery current sharing and can result in cell and battery divergence seriously affecting life. The difference in current on orbit 1251 between the three batteries is less than 0.1 A. The uniformity exists despite the difference in operating temperatures between the three batteries, given in Fig. 27, of slightly above the maximum 5 °C difference requirement. The temperature differences are due to (a) differences in thermal flow depending on space-

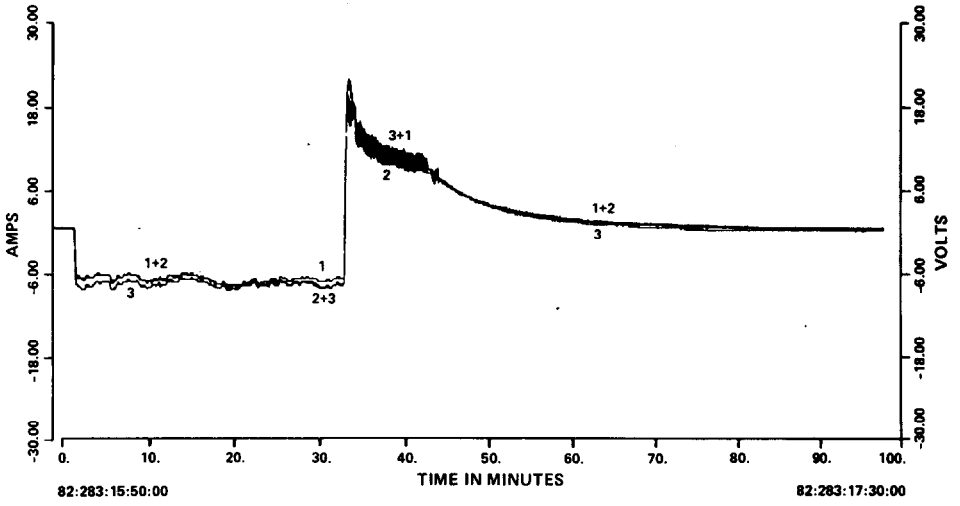

Fig. 25. Battery high current sensor, Landsat D.

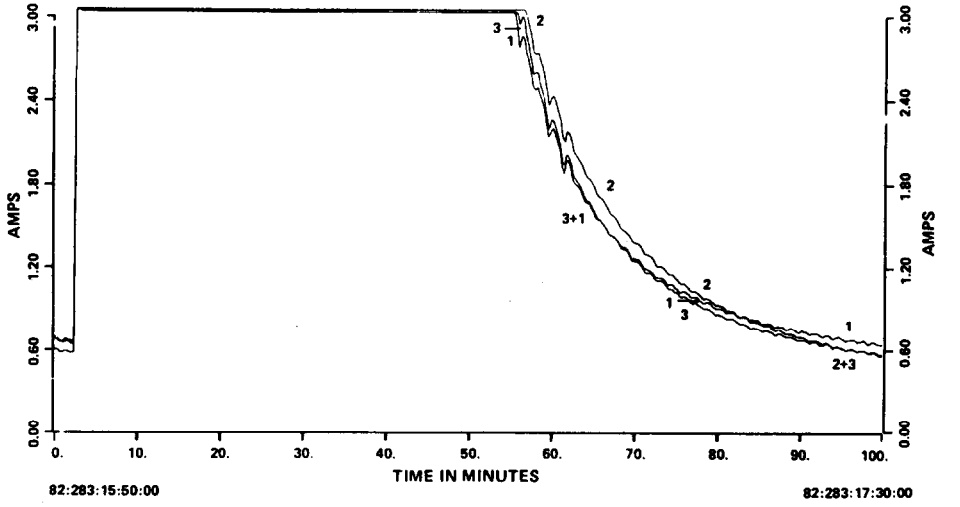

Fig. 26. Battery low current sensor, Landsat D.

craft orientation, and (b) orientation of the batteries relative to the other heat generating power system components, *i.e.*, the heat generating SPRU.

Battery differential voltage (Fig. 28) is a measure of the difference in voltage of cells 1 - 11 and cells 12 - 22 in each battery. It provides an indication of cell voltage uniformity with a battery. The original purpose was to preclude cell reversal during very deep discharges. The values for

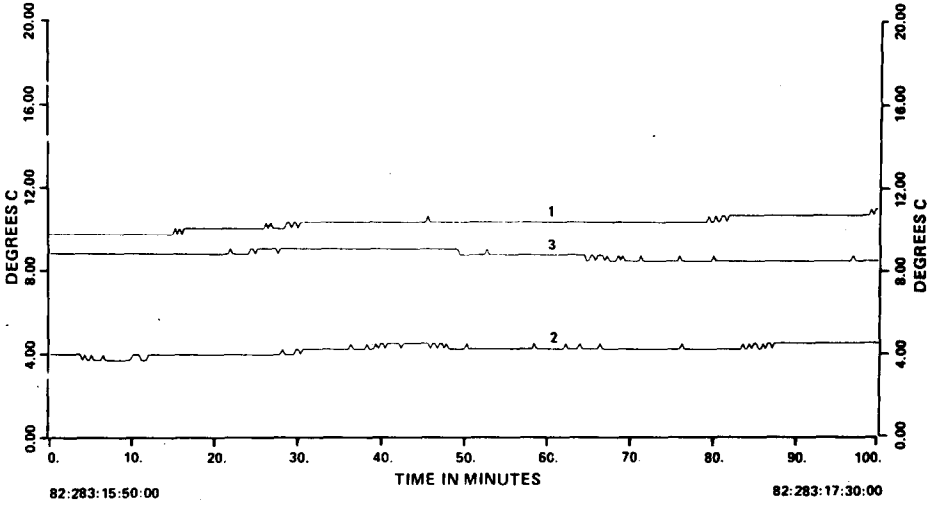

Fig. 27. Battery temperature, Landsat D.

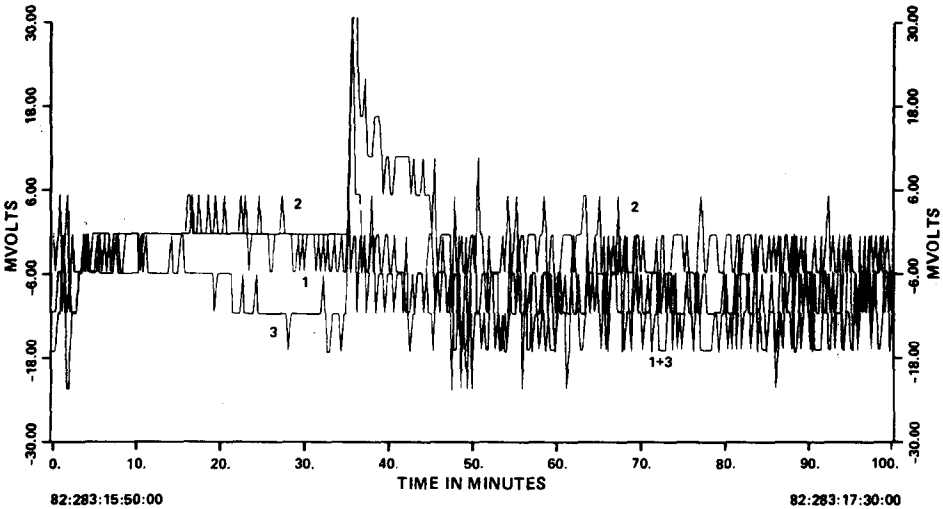

Fig. 28. Battery differential voltage, Landsat D.

batteries 1, 2, and 3 indicate a maximum ΔV of 20 mV during the orbit, except at the beginning of the day period when the maximum charge current of approximately 22 A per battery ($\sim C/2.5$) is utilized to charge the battery. Small differences in impedance can be seen, with the maximum ΔV being 30 mV when the three battery currents are identical. (The discontinuity in the data is due to telemetry readability of 3 mV.) Third electrode data are given in Fig. 29.

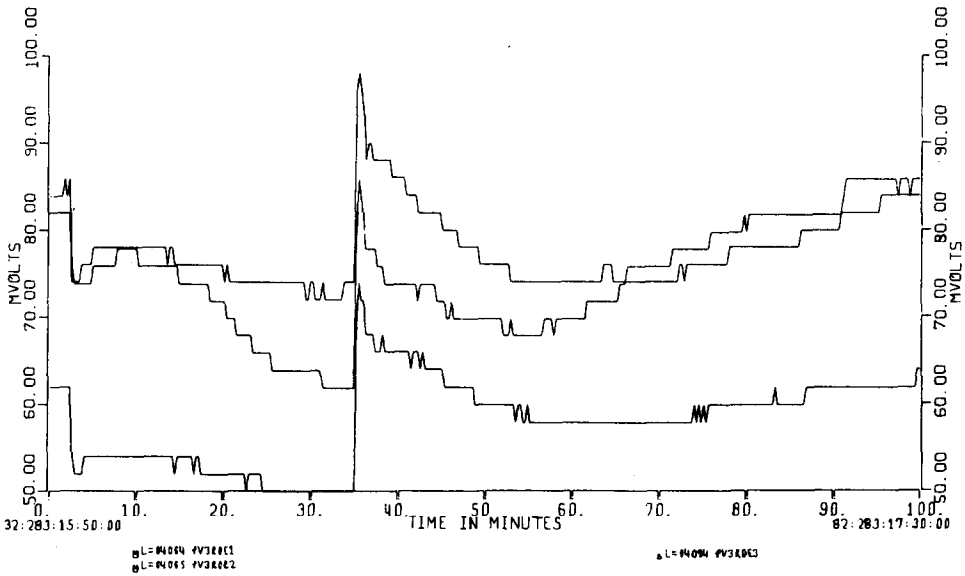

Fig. 29. Battery third electrode voltages.

Solar Max Mission results

SMM has been operating in space since February, 1980. It uses three, 20 A h batteries in the Modular Power Subsystem (MPS) instead of the three 50s of Landsat D. The 22 A peak current at the start of the daylight period is the same as for Landsat D, but for the 20 A h cells it is greater than the C rate. Despite this high rate the batteries have operated uniformly for almost three years. The current sharing of the three batteries on orbit 14 646 is given in Fig. 30. Some changes have taken place in the battery characteristics over the near three years of operation. One example is that, on orbit 13 702, the differential battery voltage increased to approximately 60 mV (see Fig. 31). The charge voltage limit was at NASA V_T Level 4 [5, 6] (1.435 V/cell at 5 °C) for the past 10 months because of a relatively low (14%) depth of discharge and the need to avoid overcharge (overheating) by minimizing the ratio of ampere hours-in to ampere hours-out. The unusual ΔV was evident at the end of discharge and beginning of charge only on battery No. 3, the hottest of the three in the SMM Modular Power Subsystems (MPS). Increasing the V_T level to 5 (1.455 V/cell at 5 °C) eliminated the high ΔV and it returned to the 20 mV maximum seen earlier (Fig. 32). This is consistent with the view that a cell/battery is a voltage device and must be charged to a high enough voltage to maintain full charge. The higher V_T resulted in placing the cells and batteries in more uniform charged condition, thus a more uniform discharge.

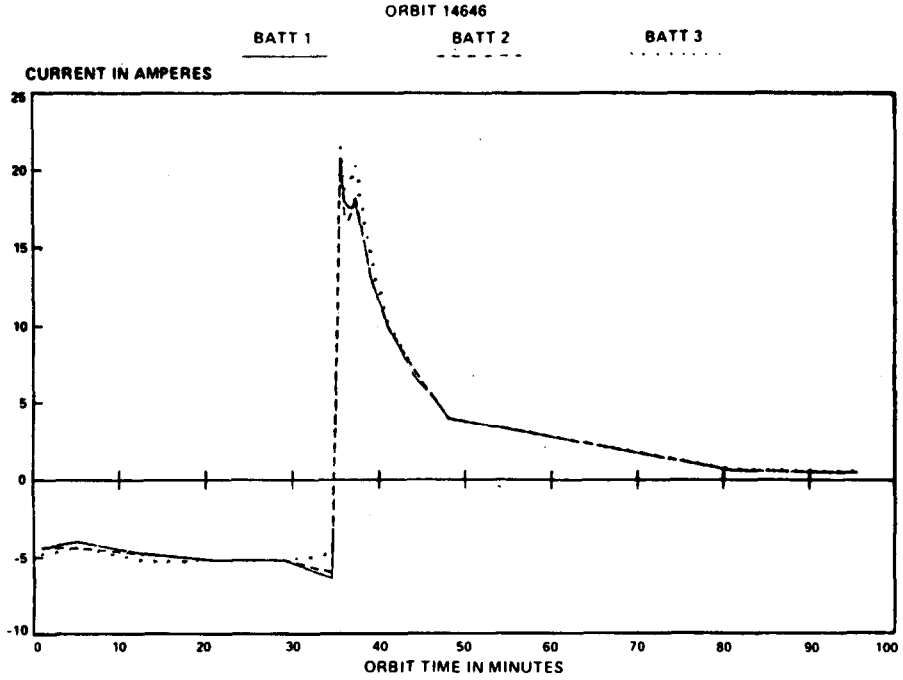

Fig. 30. SMM battery current sharing characteristics.

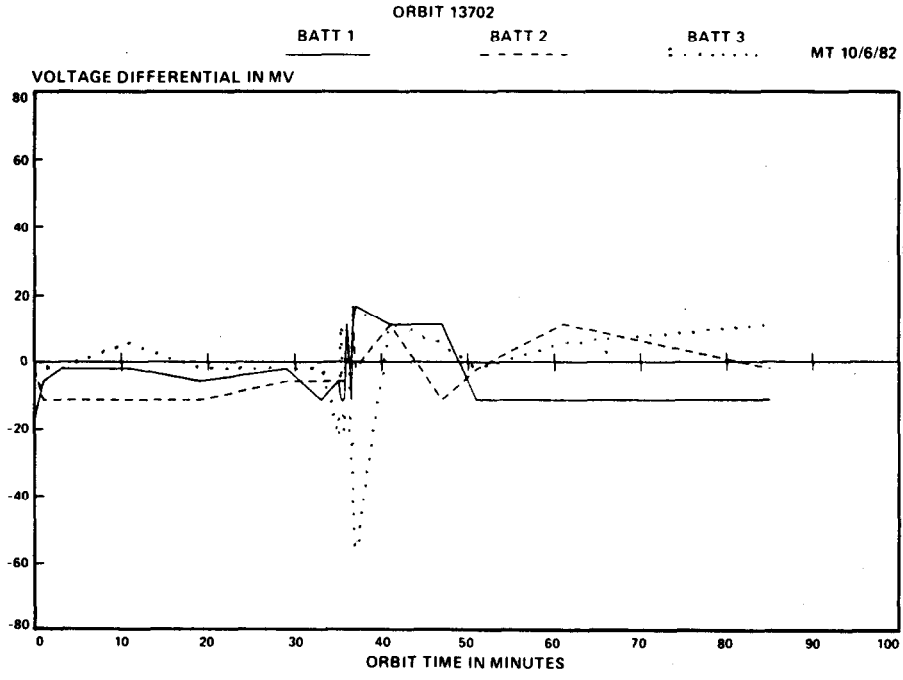

Fig. 31. SMM battery differential characteristics, orbit 13 702.

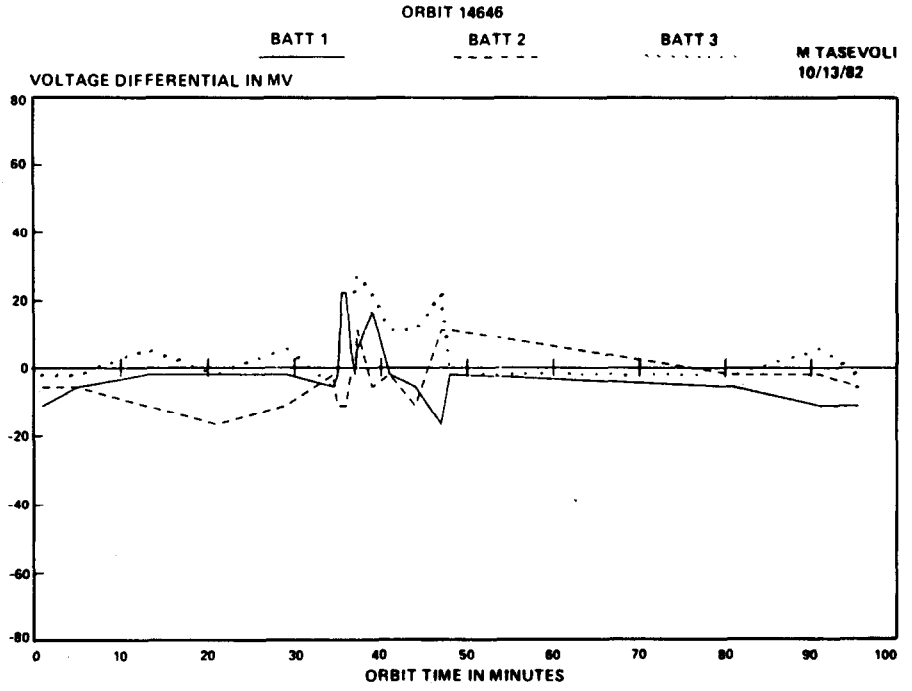

Fig. 32. SMM battery differential voltage characteristics, orbit 14 646.

Conclusions

The information presented here provides evidence that NASA Standard Cell design, which emphasized uniformity throughout the manufacturing, test, and battery assembly phase, can operate uniformly for extended periods of time in orbit. This is based on current sharing, ΔV, and voltage data for SMM and Landsat D taken over the past three years. Further, the three batteries, with such uniform operating characteristics, can be connected in parallel on the same bus for both charge and discharge and perform almost identically for extended periods with little or no adjustment in orbit. A final factor is that, with the uniform cell characteristics, only 25 cells need be available to select 22 cells for each battery. Even more amazing is the fact that 22 cells were selected based on cell manufacturer's data alone, a procedure that could only be instituted with confidence with cells of uniform properties, such as those made in accordance with the NASA Standard Cell design assembled into batteries in accordance with the NASA Standard Battery design.

Acknowledgments

This work was performed while the author was a member of the Technical Staff at Goddard Space Flight Center. The author acknowledges the

efforts of many persons there, especially F. Ford and D. Baer of the Electrochemical Applications Branch. In addition, the support of GSFC's Multimission Modular Spacecraft (MMS), Solar Max, and Landsat D Project Offices, and the information supplied by Donald Webb of McDonnell Douglas Astronautics Company, is greatly appreciated.

The preparation and publication of this paper was supported by the Jet Propulsion Laboratory, California Institute of Technology, under contract to the National Aeronautics and Space Administration.

References

1 The NASA Standard 20 A h Nickel Cadmium Battery Manual, *NASA CR 166 700* (Rev. A, 5/18/80), prepared by McDonnell Douglas Corp. under Contract NAS-5-23844.

2 The NASA 50 A h Nickel Cadmium Battery Manual, *NASA CR 166 701* (Rev. A, Feb. 1981), prepared by McDonnell Douglas Corp. under NASA Contract NAS-5-23844.

3 The specification for Aerospace Nickel–Cadmium Cells, *Spec. No. 74-15000*, Jan. 1974. With Amendments of March, 1975.

4 G. Halpert, A Screening and Selection Method for Nickel–Cadmium Cell plates, *GSFC X Doc. No. X-735-70-225*, April, 1970.

5 Multimission Modular Spacecraft (MMS) Modular Power Subsystem (MPS) Battery Storage and Operating Procedures, *MMS Doc. No. 408-2101-0002*, Feb. 1982.

6 Specification for the NASA Standard 20 A h Spacecraft Battery and 50 A h Spacecraft Battery, *GSFC Specification S-711-16, Rev. B*, Sept. 1980.

7 F. E. Ford, C. F. Palandati, J. F. Davis and C. M. Tasevoli, The Characteristics and Limitations of the MPS/MMS Battery Charging System, *NASA TM 81983*, November, 1980.

8 Qualification Evaluation Tests of 20 A h Sealed Nickel Cadmium Cells, Evaluation Program for Secondary Spacecraft Cells, Contract S-57075 AG, *Naval Weapons Support Center (NWSC) Rep. No. WQEC/C 83-133*, June 7, 1983.

9 Twentieth Annual Report of Cycle Life Test, Evaluation Program for Secondary Spacecraft Cells, Contract C-13105D, *Naval Weapons Support Center (NWSC), Crane, Ind., Rep. No. WQEC/C 84-5*, Jan. 19, 1984.

10 G. Halpert, A Comparison of Charge Control Results for Sun Oriented Versus Fixed Array Missions, GSFC Battery Workshop, November 17, 1982.